Journal of Medical and Biological Engineering (2019) 39:806–815
https://doi.org/10.1007/s40846-019-00462-1

ORIGINAL ARTICLE

Optimization of Recurrence Quantification Analysis for Detecting the Presence of Multiple Sclerosis

Simona Carrubba[1] · **Clifton Frilot 2nd**[2] · **Andrew A. Marino**[3]

Received: 12 August 2018 / Accepted: 15 January 2019 / Published online: 30 January 2019
© Taiwanese Society of Biomedical Engineering 2019

Abstract

Purpose The visual patterns in recurrence plots of time-series data can be quantified using recurrence quantification analysis (RQA), a phase-space-based method. The ability to quantitate recurrence plots affords the possibility of using them to solve central biomedical problems, for example detecting the presence of neurological diseases. Our goal was to assess this application by statistically comparing the values of plot-based quantifiers of electroencephalograms (EEGs) from patients having multiple sclerosis (MS) with values from the EEGs of control subjects.

Methods First, employing a model system consisting of the addition of known deterministic signals to the EEG of normal subjects, we empirically identified the embedding conditions that facilitated detection of the effect of the addition of the signals. Second, we used the conditions thus identified to compare EEGs from 10 patients with MS and 10 age- and gender-matched control subjects, using seven standard recurrence-plot quantifiers.

Results We identify embedding dimension of 5 points and time delay of 5 points as conditions that maximize the ability of RQA to detect the presence of deterministic activity in EEGs time series sampled at 500 Hz. The values of the RQA quantifiers computed from the EEGs of the MS patients were significantly greater than the corresponding values from the controls, indicating that the presence of the disease was associated with detectable changes in the EEG (family-wise error $< 0.05\%$).

Conclusions Recurrence plots detected the occurrence of alterations in EEGs associated with the presence of MS, indicating a decreased complexity (increased order) of brain electrical activity associated with brain disease.

Keywords Recurrence plot · Nonlinear modeling · Electroencephalogram · Multiple sclerosis

1 Introduction

Brain electrical activity is a time-dependent voltage measured on the scalp—the electroencephalogram (EEG)—consisting of an instantaneous sum of electronically propagating contributions from numerous neuronal networks, each of which exhibits intra- and inter-network nonlinear interactions. Time averaging and spectral analysis are commonly used to obtain physiological or diagnostic information from the electroencephalogram. The range of applicability of both methods is limited by their implicit assumption that the EEG is produced by linear processes in the brain. Analysis techniques recently developed to study nonlinear physical systems may be useful for obtaining information from the EEG not previously available [1]. One promising approach involves the evaluation of recurrence plots computed from mathematically transformed EEGs [2, 3].

Recurrence is a fundamental property of law-governed systems that change with time. Recurrent behavior of complex systems like the brain is typically unrecognizable by direct inspection of the time course of the signal, which appears to be random. But when such signals are embedded mathematically in a hyperdimensional phase space, the presence of law-governed activity can be visualized in two dimensions by means of a recurrence plot [4]. To facilitate quantitative analysis of the plots, Webber and Zbilut defined plot quantifiers based on the number and geometry of the points they contained [5], and took the important step of recognizing that their novel

✉ Simona Carrubba
scarrubba@mercyhurst.edu

[1] Department of Physics, Mercyhurst University, 501 E. 38th St, Erie, PA 16546, USA

[2] School of Allied Health Professions, Louisiana State University Health Sciences Center, Shreveport, LA 71130, USA

[3] Department of Neurology, Louisiana State University Health Sciences Center, Shreveport, LA 71130, USA

procedure, called recurrence quantification analysis (RQA), could be applied to time series derived from biological systems [6], which are invariably energetically open and nonstationary. They used their method to make various inferences regarding lung and muscle physiology [7]. Others used RQA to describe postural control [8], help diagnose heart disease [9] and cognitive impairment [10], characterize sleep apnea [11–13], predict the onset of an epileptic seizure [14], and rationalize inferences regarding sensory transduction of somatic stimuli [15–17].

Here we were interested in the use of RQA of EEG signals as the basis of a diagnostic test for the presence of neurological diseases. Our hypothesis is that some of the neural networks are affected by the presence the disease, resulting in dynamical changes in the contribution they make to the signal recorded on the scalp. If recurrence quantifiers reliably differed in the presence and absence of a particular disease, the presence of the disease could be inferred from the value of the quantifiers in relation to those of appropriate controls. Our goal was to assess this application by statistically comparing the values of RQA quantifiers of electroencephalograms (EEGs) from patients having multiple sclerosis (MS) with values from the EEGs of control subjects.

Multiple sclerosis is as an immune-mediated disease of the human central nervous system (CNS) that can affect any part of the brain and any cognitive function; signs and symptoms are unique to each patient and vary widely, depending on the amount of nerve damage and which nerves are affected. The most common MS diagnostic methods are magnetic resonance imaging, analysis of cerebrospinal fluid and measurement of evoked potentials, which are invasive and/or expensive [18]. EEG alone is not diagnostic, but nonlinear methods may be useful as a part of the clinician's overall diagnosis [19].

Our first aim was to find RQA parameters that would facilitate detection of the general kind of determinism we suspected might be associated with the presence of neurological diseases; we approached this task by employing a model system consisting of the addition of known deterministic signals to baseline EEGs and determined the parameter choices that best permitted detection of the added nonlinear determinism. Our second aim was to use the analytical conditions thus identified to assess the application of RQA to detect the putative changes in brain electrical activity associated with the presence of multiple sclerosis.

2 Methods

2.1 Subjects and EEG Measurements

Patients with multiple sclerosis were recruited from the outpatient neurology clinic. Inclusion criteria were: definite MS [20] with a relapsing–remitting course, but in remission; Expanded Disability Status Scale (EDSS) score ≤ 3.0 [21] for at least 3 months prior to inclusion in the study; absence of acute relapses and intravenous corticosteroid treatment for at least 60 days before inclusion in the study. The criteria resulted in the identification of 10 patients who volunteered to participate in the study, all of whom were females. The average age of the patients was 33 years (range 18–52 years). The subjects in the control group were recruited from the general population; the group consisted of ten gender- and age-matched females who had no medical complaints (average age 34 years, range 24–53 years). Written informed consent was obtained from each participant. The institutional review board at the Louisiana State University Health Sciences Center approved all experimental procedures.

Our approach was based on the theory that the EEG signal is an instantaneous sum of electrical contributions propagating from numerous neuronal networks. By hypothesis, some networks were affected by the presence of disease resulting in dynamical changes in their contributions to the signal recorded on the scalp. The recurrence method characterizes the global dynamical activity of the brain, thus, it could probe alterations in brain electrical activity from any recorded EEG derivations. EEGs were recorded continuously for 10 min from O_1, O_2, C_3, C_4, P_3, and P_4 derivations (International 10–20 system) referenced to linked ears, using gold-plated electrodes attached to the scalp with conductive paste; electrode impedances were less than 10 kΩ. During recording of the EEG the subjects sat in a darkened room on a comfortable chair with their eyes closed. The signals were amplified (Nihon Kohden, Irvine, CA), analog-filtered to pass 0.5–35 Hz, sampled at 500 Hz, and analyzed offline.

2.2 Recurrence Quantification Analysis

Use of RQA to analyze brain electrical activity involves phase-space embedding of EEG epochs, calculation of the corresponding recurrence plots, and quantification of the plots using an appropriate nonlinear quantifier. Briefly, digitized EEG epochs of length L were embedded in a multidimensional phase space employing an embedding dimension D and a time delay of τ points to produce a number N of time-lagged D-dimensional vectors, where $N = L - \tau(D-1)$. The sequence of the N vectors $(x_1, x_2, \ldots, x_N)$ corresponds to a trajectory in the phase space. The trajectory is represented in a two-dimensional plot called a recurrence plot [4]. In practice a recurrence plot $RP_{i,j}$ is obtained by plotting a point in two-dimensions at the location addressed by (i, j) whenever the ith and jth state vectors were near. Two states (x_i, x_j) are near ("or recur") if they occur within an m-dimensional spherical volume of fixed radius ε. Points in the recurrence plot correspondent to near states are called recurrence points.

$$\mathrm{RP}_{\mathrm{i,j}}(\varepsilon) = \Theta\left(\varepsilon - \left\|x_i - x_j\right\|\right)$$

where $\Theta(\cdot)$ is the Heaviside function, and $\|\cdot\|$ a norm used to calcite the distance between two state vectors in phase space. The Euclidean norm was used for calculating distances: states were considered recurrent when they were within 15% of the distance such that all points were recurrent.

Seven measures have been described for characterizing a recurrence plot [7, 22]. The principal variable is percent recurrence, $\%R$, which enumerates the number of points in the recurrent plot. $\%R$ is defined as the number of recurrent points in the plot divided by the total number of point locations (places where a point could have been placed) excluding the main diagonal (where each state recurs with itself).

$$\%R = \frac{1}{N(N-1)} \sum_{i \neq j=1}^{N} \mathrm{RP}_{\mathrm{i,j}}(\varepsilon)$$

By definition, $\%R$ measures the amount of law-governed activity in a signal in the sense that higher values are interpreted to mean that the system which produced the signal is more predictable. Nevertheless $\%R$ is only a relative measure of the amount of recurrence present because its value depends on the definition of nearness (the stricter the definition the smaller the value of $\%R$).

The remaining six RQA quantifiers are defined on the basis of geometrical features of the points in the plot which depends on length, number and distributions of diagonal lines and vertical lines in the RP. Trend (*TD*) is the regression coefficient for the relationship between the density of recurrent points on a line parallel to the main diagonal of the plot and the distance from that diagonal; *TD* was initially intended to detect linear drift in a signal. Percent determinism ($\%D$) is the percentage points in the plot that form diagonal lines. The number of adjacent points that form a line l is an adjustable parameter. Adjacent diagonal points in a plot correspond to successive states of the system, which is generally assumed to have occurred as the result of a deterministic law; in this sense $\%D$ is also a measure of the amount of the law-governed activity in a signal. Max Line (*ML*) is the length of the longest diagonal line; larger *ML* values are associated with more periodic systems. Entropy (*ET*) is the Shannon information entropy of the distribution of diagonal lines, measured in bits; larger *ET* values imply more complex dynamical activity. Percent Laminarity ($\%L$) is the percentage of points in the plot that form vertical lines. Trapping Time (*TT*) is the average length of the vertical lines. We treated the geometrical measures as equally relevant and mutually independent variables.

2.3 Modeling Procedure for Optimizing Signal Detection

Implementation of RQA requires choosing specific values for various adjustable parameters, including embedding parameters (phase space dimension and time delay), recurrence method parameters (recurrence nearness, deterministic line, recurrence epoch), and time series sampling frequency. Presently there is little systematic information available concerning the particular choices of the parameters of the recurrence method that best permit characterization of the human EEG. Still more troublesome, theoretical rules for choosing embedding parameters offer no definitive answers regarding the choice of specific values for characterizing nonstationary time series [23].

We, therefore, employed a modeling procedure to identify empirically optimal embedding conditions for detecting the presence of known determinism in the EEG. For this purpose, we added 1-s segments of law-governed activity (V_{alt}) in a point-by-point faction to baseline epochs of EEG (V_{org}), and then we used RQA to systematically investigate the conditions that optimized our ability to detect the added signals by comparing the augmented epochs ($V_{aug} = V_{org} + V_{alt}$) with baseline epochs ($V_{org}$).

Two kinds of deterministic signals were employed. The first signal consisted of segments obtained from a solution of the Lorenz equations with parameters in the chaotic domain (10, 28, 2.67 for σ, r, and b, respectively), [23]. The second signal consisted of segments of a 10-Hz signal, which is a prominent frequency in the human EEG. Each added segment was unique (different segments of the Lorenz equations, phase-randomized segments of sine wave).

The modeling analysis was performed using S/B of 0.1, 0.4, and 1.0, where S is the root-mean-squared (rms) value of the deterministic segment added to the EEG and B is the rms value of the baseline EEG epoch to which it was added. A number $N = 100$ of free-artifact epochs from each derivation were used for in the modeling procedure. The modeling analysis was repeated in ten independent EEG data sets recorded from healthy subjects using time delays (τ) of 1–5 points, embedding dimensions (D) of 3–7, line values of 2 and 20. A total of 9000 simulations (10 subjects × 6 derivations × 5 time delays × 5 embedding dimensions × 2 line parameters × 3 signal-to-baseline ratio) were run in the modeling study. The results of the modeling procedure were independent of the particular EEG electrode, therefore data from derivation O1 are displayed in the modeling results. All the calculations were carried out using a custom code (Matlab, Mathworks, Natick, MA).

2.4 Clinical Study

Using RQA embedding conditions optimized for maximizing the detection of the Lorenz and random-sine determinism, we compared MS and control group data. The design of our study incorporated the assumption that electrical signals recorded from different derivations carried essentially the same dynamical information, and that any differences between specific electrodes was due to variations in EEG baseline activity and did not carry specific physiological information. Thus, for each participant we computed the mean values of RQA variables from each derivation (using free-artifacts 1-s epochs/signal) and then averaged the results across all six electrodes to form the grand means which were used in the planned comparisons.

2.5 Statistical Analysis

The model data was evaluated using the unpaired *t* test to compare baseline control EEGs epochs and augmented EEGs formed by point-wise addition of the nonlinear signals V_{aug}. The clinical data was evaluated using the unpaired t test to compare the MS and control groups. In both studies, the pair-wise significance level was $p < 0.05$. To provide protection against family-wise error when evaluating the hypothesis that the clinical groups differed, we required that the statistical comparisons involving at least two of the seven RQA variables were pair-wise significant at $p < 0.05$, which resulted in a family-wise error rate (P_{FW}) of less than 0.05. As a control procedure the modeling and clinical data was also analyzed by time averaging and spectral analysis, using the relative power in 0.5–7 Hz, 8–12 Hz, 13–20 Hz, and 21–35 Hz.

3 Results

3.1 Model Study

The EEG was highly nonstationary (Fig. 1). The histogram of the first zero of the autocorrelation function values—a measure of the correlation between observations of a time series—computed for 1-seconds EEG epochs indicated that the statistical properties of the EEG were nonstationary (Fig. 1a). Estimation of the embedding time delay based on computation of the first minimum of the average mutual information (AMI), a method which provided more stable results for the computation of time delay than the method based on autocorrelation function [24], also produced values of the parameter that changed significantly from second to second (Fig. 1b). Nevertheless the EEG contained law-governed activity as revealed by the presence of characteristic patterns in their recurrence plots (Figs. 2a and 3a, top panels). Mathematically certain signals from the Lorenz equations also appeared irregular, but exhibited more pronounced patterns in the recurrence plots (Fig. 2a, center panel). Sine signals are periodic and exhibited distinct regular patterns in the recurrence plots (Fig. 3a, center panel). When a randomly chosen 1-s Lorenz segment (V_{alt}) was added to a 1–s epoch of EEG (V_{org}) obtained from the O_1 derivation of a clinically normal subject such that V_{alt} had an rms value 40% of that of V_{org}, the linear sum (V_{aug}) typically resulted in RP similar to those of the original epoch (Fig. 2b, bottom panel). Similar results were found when the added deterministic signal was a 10-Hz sine wave (Fig. 3b, bottom panel).

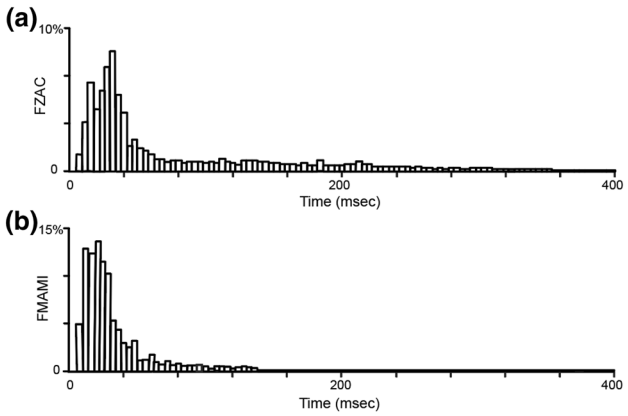

Fig. 1 Time delay estimation. Histograms of **a** the first zero of the autocorrelation function (FZAC) and **b** the first minimum of the average mutual information (FMAMI). FZAC and FMAMI were determined second-by-second from 10 min EEGs recorded from 6 derivations from 10 healthy subjects (~36,000 s, Fs = 500 Hz). The results were divided into 4-ms bins (time-delay = 2), averaged, and normalized

Although the addition of segments of deterministic signals to EEGs typically produced relatively small changes in the recurrence plots, statistical analysis across free-artifact trials ($N = 100$) confirmed that the added determinism had a statistically significant effect on the RQA quantifiers (Fig. 4). The optimal delay depended on the nature of the determinism, as evidenced by the relative inefficiency of $\tau = 1$ for detecting the effect of adding the Lorenz signal, but not for detecting the effect of adding the sine signal. For Lorenz determinism, detection was more efficient at a line of 2 compared with 20; in contrast, a higher value of the line parameter did facilitate detection of the sine determinism. For the Lorenz signal, Trend and Max Line were ineffective in detecting any change under all embedding conditions. For the sine, Max Line was ineffective, but trend resulted in detection in all three data sets for almost all embedding conditions. When the added determinism was detected, the numerical values of the RQA variables were less for V_{aug} compared with V_{org}; the exceptions were trend in connection

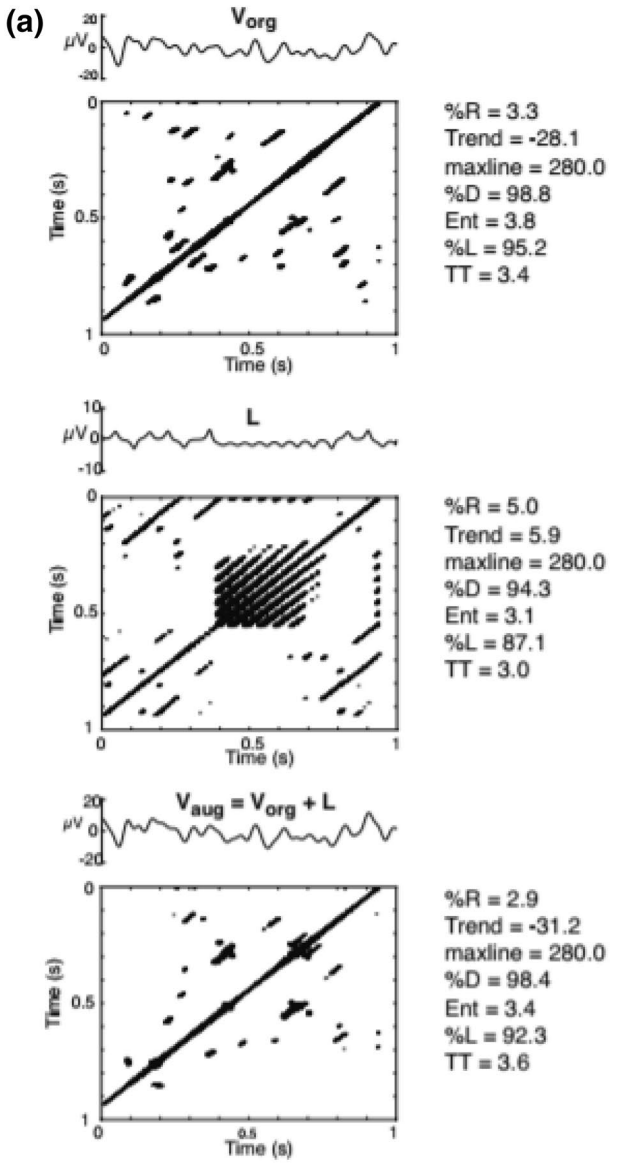

(b)

	V_{org}	L	V_{aug}
%R	5.6	7.25	4.7
Trend	-34.1	-36.3	-30.9
maxline	274.3	221.4	276.4
%D	98.8 (51.1)	95.0 (54.2)	98.5 (52.3)
Ent	3.9 (3.4)	3.3 (4.0)	3.7 (3.1)
%L	94.1 (8.6)	89.7 (6.9)	92.0 (4.6)
TT	4.9 (12.1)	4.9 (9.0)	4.2 (7.9)

Fig. 2 Detection of added Lorenz segments. **a** V_{org}, original one-second epoch of EEG (top panel); V_{alt}, Lorenz segment (L), (rms 40% of V_{org}), (center panel); V_{aug}, point-wise sum of V_{org} and V_{alt} (bottom panel). Dimension 5, Time delay 5 points (10 ms), Line 2. **b** Average results. Results for line = 20 shown in parentheses

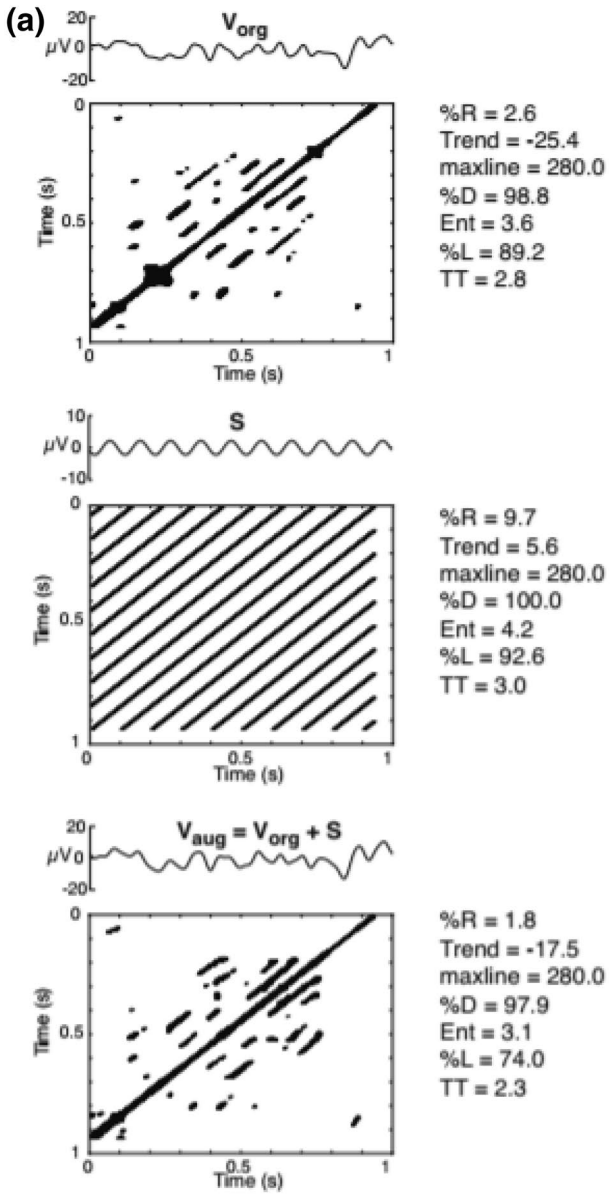

(b)

	V_{org}	S	V_{aug}
%R	5.6	9.6	4.3
Trend	-34.4	5.3	-26.8
maxline	274.3	279.3	276.6
%D	98.8 (51.1)	100.0 (99.2)	98.9 (51.0)
Ent	3.9 (3.4)	4.7 (4.6)	3.9 (3.1)
%L	94.1 (8.6)	92.4 (0)	92.3 (2.8)
TT	4.9 (12.1)	3.0 (-1.0)	3.9 (4.6)

Fig. 3 Detection of added sine segments. **a** V_{org}, original 1-s epoch of EEG (top panel); V_{alt}, sine segment (S), (center panel); V_{aug}, point-wise sum of V_{org} and V_{alt} (bottom panel). Dimension 5, Time delay 5 points (10 ms), Line 2. **b** Average results ($N = 100$ epochs). Results for line = 20 shown in parentheses

with sine determinism in all the analyzed sets, and Max Line in connection with both Lorenz and sine determinism. A wide range of embedding conditions was considered in the modeling studies. Although various combinations of the embedding conditions permitted detection of the effect of addition of the determinism, and variations occur among

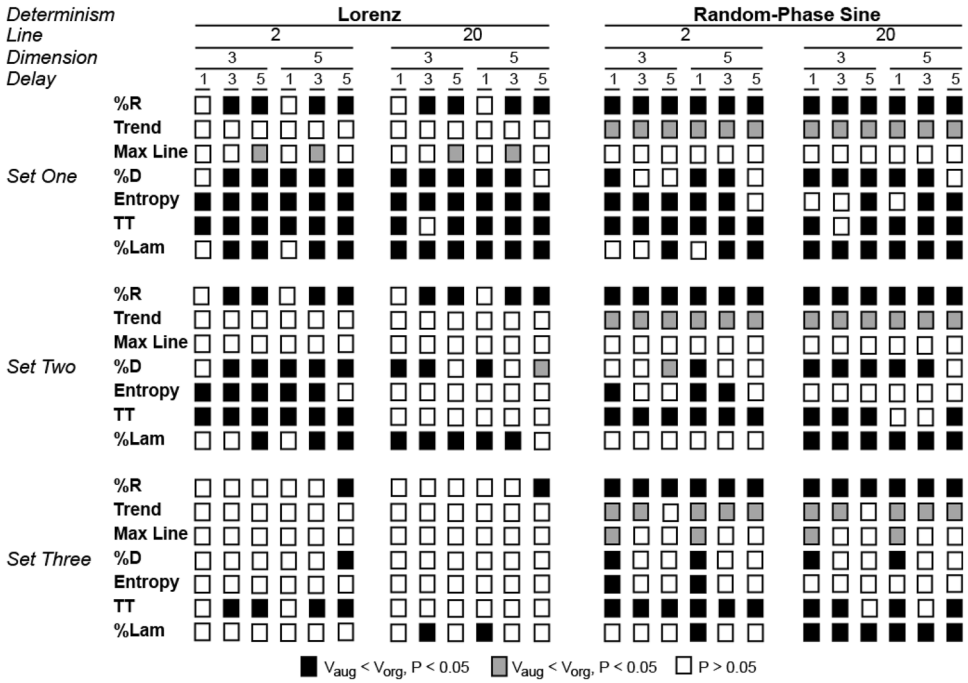

Fig. 4 Detection of addition of deterministic segments to the EEG. Either Lorenz or randomized-phase sine one-sec segments (left and right panels, respectively) were added to baseline EEG epochs (N = 100) and the computed RQA variables were compared between the augmented and original signals at each of the indicated embedding conditions for line values of 2 and 20, using the paired t test (S/B = 0.4). Comparisons from three independent data sets are shown. Conditions that resulted in pair-wise significant differences are indicated by shaded squares. Dark (light) shading indicates that the value of the RQA variable for the augmented signal was less (greater) than that of the original signal

subjects, we found that the value of 5 for embedding dimension and time delay permitted optimal detection of the added determinism. Only $D = 5$, $\tau = 5$ resulted in detection of both signals in more than one RQA variable in all the ten analyzed data sets (Fig. 4 shows exemplar results from 3 independent data sets). The detection of added determinism did not depend on the particular derivation (results from O1 derivation are displayed in Fig. 4).

The overall modeling procedure was repeated twice after adjusting the rms value of the added signal to equal either 10% or 100% of the corresponding EEG epoch. At 100%, the presence of added determinism was detected by all RQA variables (except Max Line) in all embedding conditions; at 10%, it was not detected in any of the tested conditions.

Spectral analysis was ineffective in detecting the deterministic added signals with the exception of alpha relative power for detecting sine wave using signal-baseline-ratio ratio 1.

3.2 Clinical Study

Using the optimal embedding conditions from the model ($D = 5$, $\tau = 5$), we analyzed the EEGs from patients with MS and from control subjects using line values of 2 and 20, and found 7 pair-wise significant comparisons among 11 independent tests, indicating that the brain electrical activity of patients with MS different from that of controls (Fig. 5). The grand mean ± SD of *%R* for the patients with MS was 6.6 ± 1.3%, compared with 5.1 ± 1.3% in the normal group (P = 0.017). The other two line-independent quantifiers (Trend and Max Line) were also increased ($p < 0.05$) in the MS group (Fig. 5a). Among the line-dependent quantifiers, *%D* was the only one that did not register a statistically significant difference between the MS and control groups (Fig. 5b and c). The fraction of recurrence points that formed vertical lines (*%L*) decreased greatly with increased line and, at line = 20, resulted in the loss of statistical difference between the means of the groups. In contrast, the mean length of the vertical lines (*TT*) increased when the line parameter was 20, and the difference in the averages of the two groups increased markedly.

Separate analysis using data from individual electrodes were performed, and the overall results were the same as those showed in Fig. 5 (data not shown). When the analysis was repeated after blocking on electrode derivation, as expected, inter-subject and inter-electrode variations were detected. We attributed these variations to random statistical effects due to fluctuations in the EEG background activity. The significant differences between MS and control groups were mostly observed across the central and occipital derivations (Table 1). The grand mean ± SD of *%R* for the patients with MS was 6.8 ± 2.0%, compared with 4.8 ± 1.8% in the normal group (P = 0.014). On the contrary, spectral analysis yielded no evidence of intergroup differences (Table 2).

4 Discussion

4.1 Model Results

Various analytical methods have been proposed to objectively capture physiological information in the EEG that

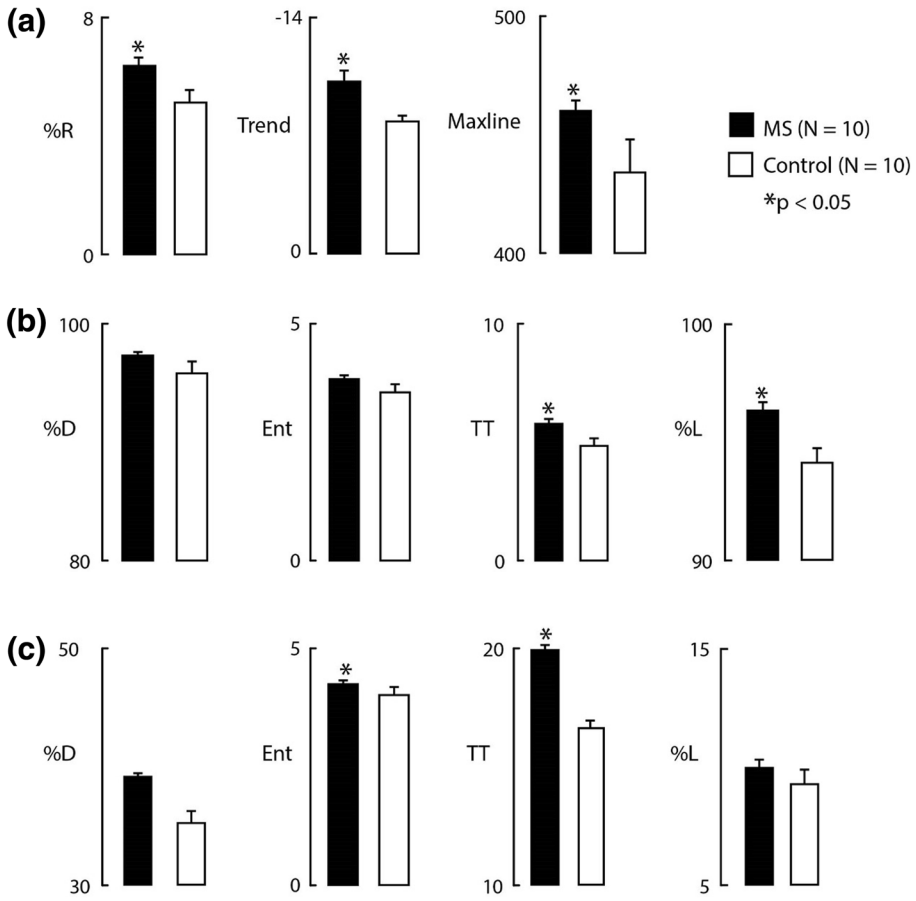

Fig. 5 Use of RQA to detect the presence of multiple sclerosis (MS) in electroencephalographic time series. **a** Line-independent variables. **b** Line = 2. **c** Line = 20. Dimension 5, Time delay 5 points (10 ms). Grand average and standard errors across all derivations

Table 1 Effect of electrode derivation on the comparison of brain electrical activity between patients with MS and normal controls, assessed using the RQA variable %R. Mean ± SE for the O, C, and P derivations

	C	P	O	Combined derivations
MS	6.8 ± 2.0	5.8 ± 1.1	7.1 ± 2.0	6.6 ± 1.3
Normal	4.8 ± 1.8	5.2 ± 1.3	5.5 ± 1.2	5.1 ± 1.3
P value	0.014	0.150	0.060	0.017

Table 2 Evaluation of electroencephalograms using spectral analysis. Relative power in four frequency intervals compared between ten subjects with multiple sclerosis (MS) and ten clinically normal subjects. Mean ± SE for O, C, and P derivations

	0.5–7 Hz	8–12 Hz	13–20 Hz	21–35 Hz
MS	50.4 ± 19.7	29.4 ± 20.3	11.6 ± 6.3	4.4 ± 2.2
Controls	60.3 ± 15.6	26.0 ± 13.7	13.6 ± 5.9	3.3 ± 2.2
P value	0.140	0.639	0.721	0.654

had been presumed to be coded in the signal ever since it was discovered. Spectral analysis has been partially successful, but it is based on the assumption that the EEG is the sum of individual stationary oscillators, which is inconsistent with the modern view of cognitive processing [25–27]. RQA, in contrast, does not assume the existence of oscillators or require that brain electrical activity be the result of autonomous differential laws. RQA is therefore independent of nonlinear dynamical theory, but this property carries with it the limitation that the parameters associated with the method, especially the embedding parameters, must be determined empirically rather than by means of theoretical rules (Fig. 1). On the other hand, a completely empirical approach is possible in which the values of RQA quantifiers of groups of biological data are compared statistically to produce biological knowledge of potentially great practical significance. We followed this approach.

Using time series of brain electrical activity to which known deterministic signals had been added, we identified $D = 5$, $\tau = 5$ as embedding conditions that maximize detection of Lorenz and random-phase sine wave signals that were added to EEG (Figs. 2, 3, 4). For several reasons, the added signals were reasonable surrogates for putative changes associated with the presence of brain disease. First, the added signals did not materially change the rms value of the original EEG segment. Thus V_{aug} and V_{org} mimicked the actual clinical situation (no difference in the rms of the EEGs of

MS patients compared with the EEG of clinically normal subjects). The power spectra of the added signals were also consistent with those of the EEG. Second, the parameter values that optimized detection of the added deterministic signals were identical to those previously reported for the detection of nonlinear EPs triggered by auditory, electromagnetic, and visual stimuli [15–17], which we interpret as evidence of the validity of the model system.

We systematically analyzed the model system data because any statistical difference between V_{aug} and V_{org} would indubitably have been the result of the added signals. We reasoned that not only would the corresponding embedding conditions be a good first choice for analyzing the EEGs, but also that the modeling would provide insight into the nature of the effect of deterministic activity on the RQA values of the baseline signal. However, we found no obvious general rules (Fig. 4). For example, low values of time delay were ineffective for detecting the Lorenz signal, but not for detecting the sine signal. As another example, Trend and Max Line values were consistently lower in the augmented EEG as compared to the EEG baseline when detecting Lorenz and random sine signals, while the other RQA variables were consistently higher. Taken together, these observations suggested to us that future studies involving attempts to develop recurrence plot analysis for disease detection might conduct a similar dimension/delay-time analysis directly involving the biological time series. Modeling might be employed in a less prominent role, for example to test a hypothesis that a particular rule of interpretation is generally valid, or to explore the possible role of RQA parameters such as radius.

4.2 Results of Clinical Study

The recurrence values computed from the EEG of patients with MS differed significantly from the corresponding control values in seven of eleven comparisons (Fig. 5). Overall, six RQA variables showed a statistical significant difference when MS and control groups were compared, and indicated a decrease in law-deterministic activity associated with the presence of the disease. Links between increased predictability (in our clinical study, higher values of RQA variables) and disease have been previously reported. EEGs in patients with Alzheimer's disease were less complex and more regular than in healthy control subjects [28, 29]. Postural instability in patients with Parkinson's disease was less complex and more rigid compared with healthy controls [30]. Ironically, %D, the RQA variable for which a dynamical meaning has most frequently been asserted, was the only variable that did not discriminate between the groups (Fig. 5). The strongly band-limited nature of the EEG is a possible explanation. The EEG is typically sampled at 100–500 Hz, and band-limited by analog filtering to 0.5–35 Hz, which produces a signal with a $\%D$ of about 98%. Thus, there is not much room for change, if the results of the intervention make the system even more deterministic.

Using conventional frequency analysis, and comparing the power spectrum across four frequency bands, we were unable to differentiate between MS and control groups (Table 2). However, other literature studies have proposed more complex spectral methods to examine cognitive dysfunction associated with multiple sclerosis [31–33] and cognitive impairment diseases [34–36].

Demonstrating that a disease group differs from a control group, on average, is a necessary but not sufficient basis for a diagnostic test, which involves a decision regarding an individual. In addition, although, recurrence method is potentially useful in conjunction with other standard diagnostic methods, its specificity to a particular disease is unknown. One possibility for improvement in the sensitivity and specificity of RQA for clinical diagnosis might be the discovery of embedding conditions that discriminate more completely between the groups. Discrimination might also be achieved by employing a discriminant function involving several RQA variables.

4.3 The Role of RQA in Medicine and Biology

Recurrence plots permit visualization of patterns encoded in a time series and, at least for stationary closed systems, the images may be interpretable in terms of the dynamics of the underlying system [4]. By using inspection alone (no information regarding governing equations), it is not possible to determine whether a plot was derived from an open or closed system, or an empirical or theoretical system. This consideration suggested to us that there is a fundamental distinction between invention of the recurrence plot (RP) by Eckmann et al. [4] and the invention of recurrence quantification analysis (RQA) by Webber and Zbilut [5]. The usefulness of RP invention is based on visualization of the plot in conjunction with other visualizations of the system's dynamical activity, for example those depicting bifurcation in the system or the presence of chaos [37]. On the other hand, we can look at RQA invention as a numerical replacement of the plot, or as a transformation of the plot into numbers, thereby facilitating hypothesis-testing, thereby permitting testing of hypotheses such as "Drug X caused more tissue damage than drug Y."

It is difficult to overestimate the potential significance of the RQA invention with regard to the analysis of biological time series, particularly extraordinarily complex series such as those generated by brain activity. The invention permits numerical characterization of recurrence (interpreted as law-governed activity) in any biological time series, and no other method is capable of doing so. The barrier that must be overcome to exploit biological applications of RQA involves

the formulation and validation of rules within which one attempts to answer the basic question "Is time series *A* different from time series *B*?" Unlike the RP invention wherein the existence of governing equations in a time series could be used to guide interpretations of a plot, the RQA invention provides no built-in interpretational standard. Such standards exist, however, in the form of basic principles of experimental design. If, for example, %R in an independent series of trials obtained from a biological system in state A differed significantly ($p < 0.05$) from the corresponding values when the system was in state B, it may be reasonable to conclude that the factor which differed between the two states was the cause of the difference in %R, in other words, that the system detected the factor. The point is that the RP and RQA inventions have markedly different advantages and disadvantages and apply in different realms. The RP invention may provide almost certain knowledge regarding the behavior of conceptual systems, whereas the RQA invention may provide imperfect but important, unique information regarding the behavior of empirical systems.

References

1. Carrubba, S., Frilot, C., Chesson, A. L., & Marino, A. A. (2007). Evidence of a nonlinear human magnetic sense. *Neuroscience, 144*(1), 356–367.
2. Frilot, C., II, Kim, P. Y., Carrubba, S., McCarty, D. E., Chesson, A. L., Jr., & Marino, A. A. (2014). Recurrence Quantification Analysis: Understanding Complex Systems. In C. Webber & N. Marwan (Eds.), *Analysis of brain recurrence* (pp. 213–251). Switzerland: Springer.
3. Schinkel, S., Marwan, N., & Kurths, J. (2009). Brain signal analysis based on recurrences. *Journal of Physiology Paris, 103*(6), 315–323.
4. Eckmann, J. P., Kamphorst, S. O., & Ruelle, D. (1987). Recurrence plots of dynamical systems. *Europhysics Letters, 4,* 973–979.
5. Zbilut, J. P., & Webber, C. L. (1992). Embedding and delays as derived from quantification of recurrence plot. *Physics Letters A, 171,* 199–203.
6. Webber, C. L., & Zbilut, J. P. (1994). Dynamical assessment of physiological systems and states using recurrence plot strategies. *Journal of Applied Physiology, 76*(2), 965–973.
7. Webber, C. L., Schmidt, M. A., & Walsh, J. M. (1995). Influence of isometric loading on biceps EMG Dynamics as assessed by linear and nonlinear tools. *Journal of Applied Physiolology, 78*(3), 814–822.
8. Apthorp, D., Nagle, F., & Palmisano, S. (2014). Chaos in balance: Non-linear measures of postural control predict individual variations in visual illusions of motion. *PLoS ONE, 9*(12), e113897.
9. Liang, Q. Z., Guo, X. M., Zhang, W. Y., et al. (2015). Identification of heart sounds with arrhythmia based on recurrence quantification analysis and kolmogorov entropy. *Journal of Medical and Biological Engineering, 35,* 209–217.
10. Timothy, L. T., Krishna, B. M., & Nair, U. (2017). Classification of mild impairment EEG using combined recurrence and cross quantification analysis. *International Journal of Psychophysiology, 120,* 86–90.
11. Song, I. H., Lee, D. S., & Kim, S. I. (2004). Recurrence quantification analysis of sleep electroencephalogram in sleep apnea syndrome in humans. *Neuroscience Letters, 366*(2), 148–153.
12. Carrubba, S., Kim, P. Y., McCarty, D. E., Chesson, A. L., Jr., Frilot, C., 2nd, & Marino, A. A. (2012). Continuous EEG-based dynamic markers for sleep depth and phasic event. *Journal of Neuroscience Methods, 208*(1), 1–9.
13. Martin-Gonzalez, S., Navarro-Mesa, J. L., Julia-Serda, G., Ramirez-Avila, G. M., & Ravelo-Garcia, A. G. (2018). Improving the understanding of sleep apnea characterization using recurrence quantification analysis by defining overall acceptable values for the dimensionality of the system, the delay, and the distance threshold. *PLoS ONE, 13*(4), e0194462.
14. Ouyang, G., Li, X., Dang, C., & Richards, D. A. (2008). Using recurrence plot for determinism analysis of EEG recordings in genetic absence epilepsy rats. *Clinical Neurophysiology, 119*(8), 1747–1755.
15. Carrubba, S., Frilot, C., Chesson, A. L., Jr., & Marino, A. A. (2006). Detection of nonlinear event-related potentials. *Journal of Neuroscience Methods, 157*(1), 39–47.
16. Carrubba, S., Frilot, C., 2nd, & Marino, A. A. (2010). Numerical analysis of recurrence plots to detect effect of environmental-strength magnetic fields on human brain electrical activity. *Medical Engineering & Physics, 32*(8), 898–907.
17. Carrubba, S., Minagar, A., Gonzalez-Toledo, E., Chesson, A. L., Jr., Frilot, C., 2nd, & Marino, A. A. (2010). Multiple sclerosis impairs ability to detect abrupt appearance of a subliminal stimulus. *Neurological Research, 32*(3), 297–302.
18. Hasan, K. M., Walimuni, I. S., Abid, H., Frye, R. E., Ewing-Cobbs, L., Wolinsky, J. S., et al. (2011). Multimodal quantitative magnetic resonance imaging of thalamic development and aging across the human lifespan: Implications to neurodegeneration in multiple sclerosis. *Journal of Neuroscience, 31*(46), 16826–16832.
19. Torabi, A., Daliri, M. R., & Sabzposhan, S. H. (2017). Diagnosis of multiple sclerosis from EEG signals using nonlinear methods. *Australasian Physical and Engineering Sciences in Medicine, 40*(4), 785–797.
20. McDonald, W. I., Compston, A., Edan, G., Goodkin, D., Hartung, H. P., Lublin, F. D., et al. (2001). Recommended diagnostic criteria for multiple sclerosis: Guidelines from the international panel on the diagnosis of multiple sclerosis. *Annals of Neurology, 50*(1), 121–127.
21. Kurtzke, J. F. (1983). Rating Neurologic impairment in multiple sclerosis: An expanded disability status scale (EDSS). *Neurology, 33*(11), 1444–1452.
22. Marwan, N., Wessel, N., Meyerfeldt, U., Schirdewan, A., & Kurths, J. (2002). Recurrence plot based measures of complexity and its application to heart rate variability data. *Physical Review E, 66*(2), 026702.
23. Abarbanel, H. D. (1996). *Analysis of observed chaotic data*. New York: Springer.
24. Fraser, A. M., & Swinney, H. L. (1986). Independent coordinates for strange attractors from mutual information. *Physical Review A, 33*(2), 1134–1140.
25. Kelly, A. M., Uddin, L. Q., Biswal, B. B., Castellanos, F. X., & Milham, M. P. (2008). Competition between functional brain networks mediates behavioral variability. *Neuroimage, 39*(1), 527–537.
26. Lewis, C. M., Baldassarre, A., Committeri, G., Romani, G. L., & Corbetta, M. (2009). Learning sculpts the spontaneous activity of the resting human brain. *Proceedings of the National academy of Sciences of the United States of America, 106*(41), 17558–17563.
27. Liu, Y., Gao, J. H., Liotti, M., Pu, Y., & Fox, P. T. (1999). Temporal dissociation of parallel processing in the human subcortical outputs. *Nature, 400*(6742), 364–367.

28. Jeong, J. (2004). EEG dynamics in patients with Alzheimer's disease. *Clinical Neurophysiology, 115*(7), 1490–1505.
29. Hornero, R., Abasolo, D., Escudero, J., & Gomez, C. (2009). Nonlinear analysis of electroencephalogram and magnetoencephalogram recordings in patients with alzheimer's disease. *Philosophical Transactions of the Royal Society A: Mathematical, Physical and Engineering Sciences, 367*(1887), 317–336.
30. Schmit, J. M., Riley, M. A., Dalvi, A., Sahay, A., Shear, P. K., et al. (2006). Deterministic center of pressure patterns characterize postural instability in parkinson's disease. *Experimental Brain Research, 168*(3), 357–367.
31. Leocani, L., Locatelli, T., Martinelli, V., Rovaris, M., Falautano, M., Filippi, M., et al. (2000). Electroencephalographic coherence analysis in multiple sclerosis: Correlation with clinical, neuropsychological, and MRI findings. *Journal of Neurology, Neurosurgery and Psychiatry, 69*(2), 192–198.
32. Leocani, L., Gonzalez-Rosa, J. J., & Comi, G. (2010). Neurophysiological correlates of cognitive disturbances in multiple sclerosis. *Neurological Sciences, 31,* S249–S253.
33. Babiloni, C., Del Percio, C., Capotosto, P., Noce, G., Infarinato, F., Muratori, C., et al. (2016). Cortical sources of resting state electroencephalographic rhythms differ in relapsing-remitting and secondary progressive multiple sclerosis. *Clinical Neurophysiology, 127*(1), 581–590.
34. Babiloni, C., Frisoni, G. B., Vecchio, F., Pievani, M., Geroldi, C., De Carli, C., et al. (2010). Global functional coupling of resting EEG rhythms is related to white-matter lesions along the cholinergic tracts in subjects with amnesic mild cognitive impairment. *Journal of Alzheimer's Disease, 19*(3), 859–871.
35. Blinowska, K. J., Rakowski, F., Kaminski, M., De Vico, F., Del Percio, C., et al. (2017). Functional and effective brain connectivity for discrimination between Alzheimer's patients and healthy individuals: A study on resting state EEG rhythms. *Clinical Neurophysiology, 128*(4), 667–680.
36. Ranasinghe, K. G., Hinkley, L. B., Beagle, A. J., Mizuiri, D., Honma, S. M., Welch, A. E., et al. (2017). Distinct spatiotemporal patterns of neuronal functional connectivity in primary progressive aphasia variants. *Brain, 140*(10), 2737–2751.
37. Iwanski, J. S., & Bradley, E. (1998). Recurrence plots of experimental data: To embed or not to embed? *Chaos, 8,* 861–871.